The effect of simultaneous local irradiation of pancreas and rectum on radiation-induced rectal toxicity: Apoptosis and fibrosis

Sei Hwan You

Department of Medicine

The Graduate School, Yonsei University

The effect of simultaneous local irradiation of pancreas and rectum on radiation-induced rectal toxicity: Apoptosis and fibrosis

Sei Hwan You

Department of Medicine

The Graduate School, Yonsei University

The effect of simultaneous local irradiation of pancreas and rectum on radiation-induced rectal toxicity: Apoptosis and fibrosis

Directed by Professor Chang Geol Lee

The Doctoral Dissertation
submitted to the Department of Medicine,
the Graduate School of Yonsei University
in partial fulfillment of the requirements for the
degree of Doctor of Philosophy

Sei Hwan You

June 2018

This certifies that the Doctoral Dissertation of Sei Hwan You is approved.

Thesis Supervisor: Chang Geol Lee

Thesis Committee Member#1: Jaeho Cho

Thesis Committee Member#2: Yun-Han Lee

Thesis Committee Member#3: Yong Chan Lee

Thesis Committee Member#4: Mee Yon Cho

The Graduate School
Yonsei University

June 2018

ACKNOWLEDGEMENTS

When it comes down, it says that it seeks the Lord! The doctoral course proceeded under very difficult conditions, but this was due to God's providence to bring the Lord closer. The word of a scholar comes to mind. "As I went up in the world, I felt a sense of separation from the Lord and grace. So I chose the road to be lowered in the world."

I was also able to come to Him through a difficult process. If it was easy to get a degree, and if it had been successful, could I proceed to the Lord? It is God's miracle that I have been able to come to this point after so many trials and errors because I am well aware of the shortcomings for climbing up the great mountain of research. I would like to thank to Jacob and Seung Hee Lee, my mother, my mother-in-law and my dear family for supporting me in prayer. I am grateful to Professor Gui-Eon Kim, Chang-Ok Suh, and all the faculty members of the Radiation Oncology Department for their support and encouragement, giving special thanks to Professor Chang Geol Lee for mentoring me with a chance to raise me when I am in need. I am also grateful to Professor Jaeho Cho, Mee Yon Cho, Yong Chan Lee, and Yun-Han Lee for their hard work for reviewing. I would like to thank Dr Joon Hyung Sohn for his practical help in the experiment. Lastly, I would like to thank Professor Jong Young Lee, Jihye Cha and other staffs at Wonju Severance Christian Hospital.

Sei Hwan You

<TABLE OF CONTENTS>

ABSTRACT ····· 1

I. INTRODUCTION ····· 5

II. MATERIALS AND METHODS ····· 9
1. Animal preparation ····· 9
2. Irradiation protocol outline ····· 9
3. Irradiation in concurrence to pancreas and rectum ····· 10
4. Irradiation planning ····· 11
5. Validation of planned irradiation ····· 12
6. Body weight and blood glucose measurement ····· 13
7. Tissue extraction and histological examination of the rectum ····· 13
8. Immunohistochemical staining for apoptosis assessment in rectal mucosa ····· 13
9. Evaluation of rectal mucosal and submucosal fibrosis by Picrosirius red staining ····· 14
10. Quantification of mRNAs for inflammation or fibrosis-related proteins ····· 15
11. Statistical analysis ····· 16

III. RESULTS ····· 17
1. Sample dosimetry of irradiation technique ····· 17
2. Change of body weight and blood glucose ····· 19
3. Histopathologic fingdings by hematoxylin-eosin staining ····· 20
4. Apoptosis in rectal mucosa estimated by cleaved caspase-3 immunohistochemical staining ····· 23
5. Fibrotic change in rectal mucosa and submucosa ····· 25
6. mRNA expression of IL-6, HIF-1α, VEGF-A, and NF-κB ····· 27

IV. DISCUSSION ····· 28
V. CONCLUSION ····· 35
REFERENCES ····· 36
ABSTRACT (IN KOREAN) ····· 41

LIST OF FIGURES

Figure 1. Schematic diagrams of rat irradiation method ·····11

Figure 2. An example of pancreatic shield and radiation planning process by a technique of irradiation in concurrence to pancreas and rectum (iCPR) ·····12

Figure 3. Changes in body weight and fasting blood glucose after irradiation ·····19

Figure 4. Changes in body weight for each group compared to sham irradiation group after irradiation ·····20

Figure 5. Changes in fasting blood glucose for each group compared to sham irradiation group after irradiation ·····20

Figure 6. Histological changes in irradiated rectal mucosa on hematoxylin-eosin staining ·····22

Figure 7. Cleaved caspase-3 positive cells on immunohistochemical staining ·····24

Figure 8. Fibrotic changes in rectal mucosa and submucosa on Picrosirius red staining ……26

Figure 9. Relative mRNA expression (real time PCR using rat-specific primers) compared to one control subject at the 1st week and the 14th week after irradiation for each group ……28

LIST OF TABLES

Table 1. Group classification for male Sprague Dawley rats and their number allocation according to radiation dose, pancreatic shielding, and time phase after irradiation 17

Table 2. Dosimetric comparison of mean doses of each contour volume for pancreatic shield (PS) and non-pancreatic shield (NPS) groups in 7 sample rats, with a 500-cGy prescription using a postero-anterior / antero-posterior X-ray ····· 18

ABSTRACT

The effect of simultaneous local irradiation of pancreas and rectum on radiation-induced rectal toxicity: Apoptosis and fibrosis

Sei Hwan You

Department of Medicine
The Graduate School, Yonsei University

(Directed by Professor Chang Geol Lee)

Purpose: Radiation exposure to pancreas can be a part of negative influences in gastrointestinal tract (GIT) radiotoxicity. The pancreas may affect the radiation-induced intestinal toxicity especially in healing process of GIT system by playing a role in the action of blood glucose, nutrition, and metabolism-related factors. Thus, it is necessary to analyze GIT toxicity with pancreatic radiation effect and verify radiation toxicity control system according to the concept of inter-organ system. For the assessment of radiation-induced GIT toxicity, a pancreatic radiation effect-related rat animal model was applied to confirm the concept of inter-organ correlation between GIT and pancreas.

Materials and methods: Eight-week-old male *Sprague Dawley* rats were irradiated by high-energy radiation. In order to verify the effect on the GIT toxicity according to pancreatic radiation effect, we applied the 'irradiation in concurrence to pancreas and rectum' technique which divided the irradiation

into the upper abdomen and the lower abdomen. The upper abdomen field contained the pancreas and the lower abdomen field contained the rectum. This technique was designed to provide the proper irradiation protocol in which the irradiated volume was maintained at a constant rate. Upper abdominal irradiation was categorized into pancreatic shield (PS) and non-pancreatic shield (NPS). After 5-Gy and 15-Gy irradiation, rectum tissue was analyzed at the 1st week (early phase, Ep) and the 14th week (late phase, Lp) with body weight and fasting blood glucose. Histopathology was estimated by hematoxylin and eosin (HE), Masson's trichrome, and Picrosirius red (PR) staining. Immunohistochemical staining for apoptosis assessment in rectal mucosa was performed with cleaved caspase-3 antibody. The mRNA expressions of interleukin (IL)-6, hypoxia-inducible factor (HIF)-1α, vascular endothelial growth factor (VEGF)-A, and nuclear factor (NF)-κB were analyzed as inflammation or fibrosis markers considering the relations among radiation dose, acute and chronic toxicities of the GIT and pancreatic radiation effect.

Results: The body weight gain failed to progress at the 1st week after irradiation, particularly in the NPS-15-Gy group versus NPS-5-Gy group ($P < 0.001$). The blood glucose level increased gradually until Lp after initial decrease at Ep. Both the weight gain and the blood glucose profile showed similar pattern in terms of temporary decrease at Ep especially for the NPS-15-Gy group. In HE staining, the inflammatory response of the 15-Gy irradiation groups was noticeable at early phase. Apoptosis in rectal mucosa was estimated by cleaved caspase-3 positive cells. Generally, the number of cleaved caspase-3-positive

cells was more frequently detected at late phase compared to early phase and this Ep-to-Lp increase was prominent in NPS-15-Gy group (P = 0.014). At Lp, for 15-Gy irradiation, this cleaved caspase-3 expression was dominant in the NPS group compared to the PS group (P = 0.024). Quantitative evaluation of mucosal and submucosal fibrosis was performed by the ratio of area occupied by collagen deposition in whole villi on PR stained image. Although there were no significant differences between the PS and NPS groups, mucosal and submucosal fibrosis progressed toward the late phase as a whole. This Ep-to-Lp increase was observed in all groups except the PS-5-Gy group. The collagen deposition tended to be greater in the NPS groups than in the PS groups in comparison with the sham irradiated control groups. Generally, the mRNA expressions of IL-6, HIF-1α, VEGF-A, and NF-κB showed a tendency to be prominent at early phase and to resolve after that, with the same radiation dose or pancreatic shielding condition. The dose-dependent pattern was typical for IL-6 (P = 0.020).

Conclusions: In this study, we investigated rectal radiation toxicity in relation to radiation effects on the pancreas. Histopathologic and biochemical status were changed along with radiation dose and time course. According to the animal model of this study, inflammation appeared mainly at early phase, and apoptosis occurred mainly at late phase, accompanied with fibrosis. Fibrosis was thought to occur earlier than expected in comparison with the control group, which was confirmed by collagen deposition increase. Despite no direct toxicity difference between the PS and NPS groups, our pancreatic shielding method may act as a

possible variable in the dose-dependent and time-related radiotoxicity of the rectum, suggesting the necessity of multi-organ effect-based approach in GIT radiotoxicity assessment.

Key words : radiation injuries, gastrointestinal tract, pancreas, nutritional status

The effect of simultaneous local irradiation of pancreas and rectum on radiation-induced rectal toxicity: Apoptosis and fibrosis

Sei Hwan You

Department of Medicine
The Graduate School, Yonsei University

(Directed by Professor Chang Geol Lee)

I. INTRODUCTION

The toxicity of gastrointestinal tract (GIT) such as stomach, duodenum, etc. in abdomino-pelvic radiotherapy is one of the main causes of prescribed treatment schedule delay, which have a negative effect on treatment outcome. Because of the characteristics of the GIT itself, pain and poor food intake caused by radiation toxicity makes it difficult to be recovered from the damage, which continues to vicious cycle in quality of life. At present, the solution for this kind of problems is very restrictive. That is, it depends on symptomatic palliation with drugs such as anti-inflammatory agents or analgesics. However, there have not been satisfactory improvements for these problems yet. It is known that proper radiation dose for tumor control is up to 60–70 Gy with

1.8–2.0 Gy daily fractions by radiation alone and at least 55–60 Gy when combined with surgery. However, practically, only 45–50 Gy is being delivered to the area of adjacent GIT because of relatively weak radiation tolerance of GIT mucosa. This means the poorer expectation for treatment results compared with the other anatomic areas. One of the main factors related to GIT toxicity is the degree of mucosal damage, which is caused by loss of balance between damage and regeneration. Apoptosis and clonogenic cell death can lead to cytokine-activated inflammatory reactions with peripheral immune cell activation, depending on the degree of injury.[1-4]

The pathogenesis of radiation proctitis has not been fully understood yet. Most of the mechanisms described are based on a fatal toxic process by high-dose radiation. However, even in this fatal toxic process, the onset of toxicity is mucosal damage, followed by late indolent connective tissue growth and regeneration process with the tissue response to ischemia.[5] Apoptosis is considered as one of the causes of mucosal damage, and mucosal tissues with relatively low turnover rates may be affected by relatively low radiation dose. Polistena et al.[1] reported that radiation dose-dependent caspase-3 expression was associated with the severity of histological damage. This acute inflammatory response with mucosal breakdown was also described by a fatal toxic mechanism. During these processes, pro-inflammatory cytokines such as interleukin (IL)-6 and nuclear factor (NF)-κB affect directly or indirectly.[4, 6, 7] In particular, IL-6 mRNA expression is considered to be an indicator of typical experimental radiation-induced GIT toxicity.

After irradiation, fibrosis and chronic inflammatory reaction may occur with crypt regeneration. It is known that vascular and endothelial cell injury may be involved in additional toxicity reactions.[8, 9] At this time, angiogenesis-related hypoxia-inducible factor (HIF)-1α and vascular endothelial growth factor (VEGF) are associated with fibrotic change of the rectum, whose expression patterns can change by time course.[10] However, the relevance of fibrosis to cytokine expressions also varied widely according each time point, which is still unclear.

Despite many experiment-based results, clinical manifestations cannot always be explained by these mechanisms. The tolerably administered dose for thoracic or pelvic GIT is about 55 Gy with 1.8–2.0 Gy daily fractions, while it is less than 50 Gy for upper abdominal GIT.[11, 12] This radiation vulnerability can be explained by the presence of the pancreas located at the center of the upper abdomen.[13-17]

Pancreatic dysfunction itself may affect a certain part of negative influences in the process of GIT damage and recovery. In one previous study, the concept of multi-system dysfunction was introduced for toxicity relationship between GIT tract and pancreas.[14] According to another study of stomach cancer radiotherapy, they presented a problem that radiation-induced GIT toxicity could be particularly associated with pancreatic endocrine damage.[16] However, there have not been sufficient follow-up studies for handling this topic.

Therefore, a comprehensive study needs to be performed including the concept of multi-organ effect in radiation toxicity.

If this multi-organ effect hypothesis is systematically established, the impact of pancreatic dysfunction upon GIT toxicity may be predicted effectively, actualizing more stable radiotherapy to GIT area. A representative study on the multi-organ effect was previously performed for the lung irradiation. Ghobadi et al.[18] reported that radiation-induced pulmonary damage can be affected by concurrent cardiac irradiation. In other words, heart-and-lung coirradiation showed different toxic mechanism from lung-only irradiation, which led to the difference of cardiopulmonary performance.

From this perspective, the effect of pancreatic radiation exposure needs to be considered in terms of inter-organ interaction. The purpose of this study was to analyze the GIT radiotoxicity associated with pancreatic radiation exposure through histopathology and immunohistochemistry for rectum tissue in a rat model. First, we examined the validity of the animal model through experimentally devised shielding system. Subsequently, radiation-induced rectal toxicity was analyzed to confirm the concept of multi-system dysfunction between the pancreas and the rectum focusing on apoptosis and fibrosis in mucosal and submucosal layer. A more gradual approach is required because the mechanism of radiation-induced rectal toxicity is still unclear. Thus, the radiation dose range was limited to the extent that mucosal apoptosis with mild inflammation can be induced. Fundamentally, histopathology of rectal mucosa

and submucosa was the main analysis target and the mRNA expression of IL-6, NF-κB, HIF-1α and VEGF-A was supplemented in terms of relevance to histopathologic findings.

II. MATERIALS AND METHODS

1. Animal preparation

Eight-week-old male *Sprague Dawley* rats (Daehan Biolink, Eumseong, Korea) were housed with drinking water, standard 5L79 diet (PMI Inc., St. Louis, MO, USA), and control of the temperature, humidity, and a 12-hour light-dark cycle. Irradiation was performed on the 7th day of the adaptation period post-arrival. The average body weight at irradiation was 250.9 ± 8.4 g. The status of rats was assessed by veterinarians, and all animal experiments proceeded after approval by the Institutional Animal Care and Use Committee (Approval number: YWC-141211-1, YWC-150519-2, and YWC-161207-1).

2. Irradiation protocol outline

X-rays of 6 MV were delivered by using a linear accelerator (Elekta Synergy, Elekta, Stockholm, Sweden). Three-dimensional planning was performed using a computed tomography (CT) (Aquillion LB, TSX-201A, Toshiba Medical Systems Corporation, Otawara, Japan) scan. The beam was delivered by a postero-anterior (PA) and antero-posterior (AP) combination in the prone position on the platform after the posture was set to be straight from the neck

vertebrae to the tail. The dose rate was 3.6 Gy/min. During CT scanning and irradiation, each rat was anesthetized via isoflurane inhalation using Small Animal Single Flow (O2) Anesthesia System (L-PAS-01, LMSKOREA Inc., Seongnam, Korea) with thorough monitoring. The rat position remained stable without fixation device.

3. Irradiation in concurrence to pancreas and rectum

The experimental technique of irradiation in concurrence to pancreas and rectum (iCPR) was devised to directly investigate whether rectal toxicity was associated with pancreatic radiation exposure. Overall, the iCPR volume included both the upper abdomen and the lower pelvis area. Figure 1A indicates schematic beam irradiation before shield application. On actual irradiation, a specially designed Cerrobend shield system was applied to the upper abdomen area in order to reflect pancreatic radiation exposure, which was divided into the pancreatic shield (PS) (Figure 1B and 1D) and non-pancreatic shield (NPS) (Figure 1C) groups by the shape of the shield block. A constant pelvic radiation field was maintained to ensure a fixed rectal dose as a main object of toxicity analysis.

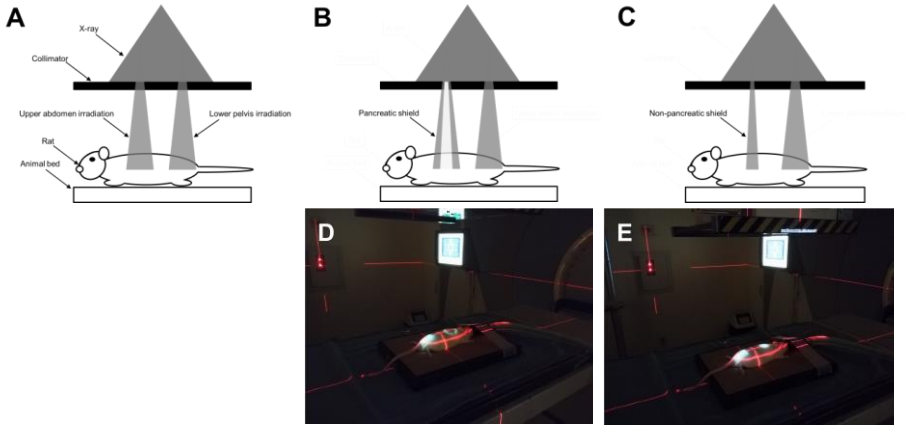

Figure 1. Rat irradiation method. (A) Schematic diagram for the 'irradiation in concurrence to pancreas and rectum (iCPR)' without shield. (B) Schematic diagram for the iCPR with pancreatic shield. (C) Schematic diagram for the iCPR with non-pancreatic shield. (D) iCPR with pancreatic shield when irradiated with visible light with shielding in the actual linear accelerator. (E) iCPR with pancreatic shield when irradiated with visible light with shielding in the actual linear accelerator.

4. Irradiation planning

Following CT scan (2 mm-sliced), major abdominal organs (liver, stomach, bilateral kidneys, and pancreas) were delineated using the Pinnacle3 planning system (Philips Healthcare, Andover, MA, USA) (Figure 2A). The central part of pancreas was contoured from the level of the renal upper pole to 8 slices upwards. The pelvic contour was delineated from the anal verge to the 18th slice upward, encompassing the whole rectum. The abdomino-pelvic contour, as a substitute for the whole body, was delineated from the diaphragm to the anal verge level. Thorax was excluded due to its small volumetric impact. NPS was set to a circular shape by homogeneous pancreatic contour expansion. PS was derived as a ring-shaped structure by additional expansion of the NPS margin (Figure 2B). The lower pelvic field was fixed to 3.4 cm × 3.6 cm-sized open rectangular shape and the whole portal area was 3.4 cm × 12.0 cm. The irradiated dose in planning was 5 Gy and 15 Gy with single fractionation, in the

low and high dose groups, respectively. Thus, the estimated dose of the rectum was 5 Gy and 15 Gy in the low and high dose group, respectively. For the central portion of the pancreas, it was to be distributed as 0 Gy, 5 Gy, 0 Gy, and 15 Gy in 5Gy-PS, 5Gy-NPS, 15Gy-PS, and 15Gy-NPS group, respectively. After dosimetric estimation for 7 sample rats, standardized prescription location (mid-depth point of the upward 7th slice from the pelvic contour upper margin) and monitor unit values for PA/AP portals (280/275 for 5 Gy and 840/825 for 15 Gy) were derived. These conditions were applied to irradiation for rectal radiation toxicity analysis (Figure 2C).

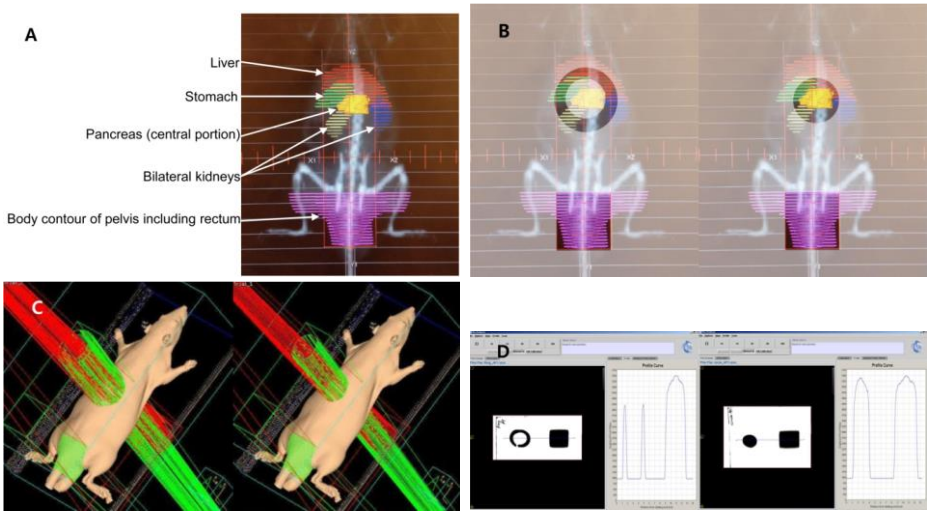

Figure 2. An example of pancreatic shield and radiation planning process by a technique of irradiation in concurrence to pancreas and rectum (iCPR). (A) Postero-anterior beam's eye view with contoured organs. (B) Actual radiation exposure after shield system application; pancreatic shield (PS, left) and non-pancreatic shield (NPS, right). (C) Rendered images of radiation planning for PS irradiation (left) and NPS irradiation (right) for postero-anterior / antero-posterior portals. (D) Dose profiles of PS (left) and NPS (right) applied to solid water phantom.

5. Validation of planned irradiation

Gafchromic EBT3 film (Ashland, Bridgewater, NJ, USA) dosimetry was

performed with a solid water phantom (RW3 Slab Phantom, PTW, Freiburg, Germany) and an ion chamber (TM 30013, PTW, Freiburg, Germany). The 6-MV X-ray was delivered perpendicularly to the film with the following conditions: 2-cm depth, 3.6-Gy/min dose rate, and 17-cm source-to-surface distance. The iCPR was applied with 5-Gy irradiation followed by dose profile confirmation for both PS and NPS (Figure 2D).

6. Body weight and blood glucose measurement

Blood glucose level and body weight were measured at 0, 1, 5, 9, 14 weeks after irradiation. Blood glucose was measured in rat tail vessel blood using a measurement kit (Accu-CHEK, Roche Diabetes Care GmbH, Mannheim, Germany) with overnight fasting (18 h).

7. Tissue extraction and histological examination of the rectum

Rats were sacrificed at the 1st week (early phase, Ep) and 14th week (late phase, Lp) after irradiation. The rectum was excised from the area where the colon exits out of the peritoneum to the anal area. The length before excision was about 3.5 cm, which was matched with the length of the longitudinal axis of the lower pelvic field. The specimens were fixed in phosphate-buffered 10% formalin and axially sectioned at the mid-point for paraffin embedding. Histopathology was estimated by hematoxylin and eosin (HE) staining on paraffin-embedded tissue sections.

8. Immunohistochemical staining for apoptosis assessment in rectal mucosa

The degree of apoptotic activity was estimated by immunohistochemical (IHC) staining for cleaved caspase-3 in mucosal layer. Following section deparaffinization and an an antigen-retrieval for 60 min, endogenous peroxidase activity was blocked by exposing the sections to an ultraviolet inhibitor for 4 min. After the reaction buffer washing, an Ultra View Universal DAB Detection Kit (Ventana Medical Systems, Tucson, AZ, USA) was used for IHC staining. The slides were incubated with monoclonal antibodies against cleaved caspase-3 (1:100, #9664, Cell Signaling Technology, Inc., Danvers, MA, USA) for 1 h at 37℃ in an autostainer (Benchmark XT, Ventana Medical Systems) and rinsed with the reaction buffer. Drops of the following reagents were applied sequentially to each slide (8 min per reagent), and rinsed again with reaction buffer: HRP UNIV MULT, DAB H_2O_2, and COPPER (Ventana Medical Systems). The slides were subsequently treated with hematoxylin for 4 min, incubated with bluing reagent for 4 min, and finally rinsed with reaction buffer. Negative control sections were also processed to evaluate for the specificity of primary antibody or background staining levels. Cleaved caspase-3 positive cells were counted in the representative mucosal area on the cross section at ×400 magnification. The degree of apoptosis in rectal mucosa was estimated by the number of cleaved caspase-3 positive cells per 100 epithelial cells in the crypts.

9. Evaluation of rectal mucosal and submucosal fibrosis by Picrosirius red staining

The fibrotic change was assessed by Masson’s trichrome and Picrosirius red

(PR) staining in rectal mucosa and submucosal area. After tissue examination by Masson's trichrome stained image, quantitative evaluation was performed by the ratio of area occupied by collagen deposition in whole villi on single-colored PR stained image. PR kit (Polysciences, Inc., Warrington, PA, USA) was used for PR staining. The single uniform red-based staining property contrasted to the unstained glandular lamina propria areas was thought to be useful for quantitative assessments. The PR-positive proportion was quantitated using an image analyzer (NIS-Elements BR version 4.30, Nikon Instruments Inc., Melville, NY, USA) with consistent intensity for each ×100 magnification image.

10. Quantification of mRNAs for inflammation or fibrosis-related proteins

For quantitative polymerase chain reaction (qPCR) analysis, tissue samples were acquired from the area adjacent to the rectal longitudinal mid-point. Because of technical limitations, the whole layer of the rectum was analyzed without mucosal tissue separation. Samples were rinsed with normal saline and stored at -80℃. RNA was extracted using the RNeasy mini kit (Qiagen, Hilden, Germany) according to manufacturer's instructions. The reverse transcription reaction was performed with 100 ng of total RNA using the ReverTra Ace® qPCR RT Master Mix with gDNA Remover (Toyobo, Osaka, Japan). Amplification of cytokine genes and 18s RNA was monitored and analyzed using the PowerUp™ SYBR Green Master Mix (Thermo Fisher Scientific Inc., Waltham, MA, USA) and the 7900HT Real-Time PCR System (Thermo Fisher Scientific Inc.). The following primers were used: IL-6 (Rn_Il6_1_SG

QuantiTect Primer Assay, Qiagen), NF-κB (Rn_Nfkb1_1_SG QuantiTect Primer Assay), HIF-1α (Rn_Hif1a_1_SG QuantiTect Primer Assay), VEGF-A (Rn_RGD:619991_1_SG QuantiTect Primer Assay), and of the endogenous control gene 18s RNA (Rn_Rn18s_1_SG QuantiTect Primer Assay). PCR amplification was carried out through 10 μL reactions, and at least 3 replicates were used for each sample. Cycling parameters: 95℃ for 10 min, followed by 45 cycles of 95℃ for 15 s and 60℃ for 60 s. Single product generation was confirmed with a melting curve analysis. Calculations of relative gene expression levels were performed using the $2^{-\Delta\Delta Ct}$ method, by normalizing them to 18s RNA expression levels. A non-irradiated 8-week-old male *Sprague Dawley* rat was used as a control object. Its rectum tissue was extracted by the same method for the irradiated groups on the 7th day of the adaptation period post-arrival.

11. Statistical analysis

The parameters of comparison were as follows: body weight, blood glucose, the number of cleaved caspase-3 positive cells, the ratio of PR-positive area, mRNA expressions according to dose (5 Gy versus 15 Gy), pancreatic shielding (PS versus NPS), and elapsed time (Ep versus Lp) after irradiation. For the comparison between the two groups of these three categories, data were assessed by the Student *t* test using SPSS version 23 (IBM, Armonk, NY, USA). A $P < 0.05$ was defined as significant. For the comparison one group to control group, the same statistical methods were applied. In comparison with the control groups, the statistical significance was classified into the following three

levels ($P < 0.05$, $P < 0.01$, and $P < 0.001$). For statistical analysis, 6 rats were allocated to each group including sham-irradiated control group at Ep and Lp (Table 1).

Table 1. Group classification for male *Sprague Dawley* rats and their number allocation according to radiation dose, pancreatic shielding, and time phase after irradiation

Group category	Control	Pancreatic shield	Non-pancreatic shield
Early phase (1 week after irradiation)			
0 Gy	6		
5 Gy		6	6
15 Gy		6	6
Late phase (14 weeks after irradiation)			
0 Gy	6		
5 Gy		6	6
15 Gy		6	6

III. RESULTS

1. Sample dosimetry of irradiation technique

Generally, the dosimetric condition of the PS group was inferior to the NPS group in terms of radiation toxicity. According to the mean doses for each contour volume, PS showed higher or equal dose distribution compared to NPS except for the pancreas. Pelvic and abdomino-pelvic contours did not show mean dose difference between the PS and NPS group (Table 2).

Table 2. Dosimetric comparison of mean doses of each contour volume for pancreatic shield (PS) and non-pancreatic shield (NPS) groups in 7 sample rats, with a 500-cGy prescription using a postero-anterior / antero-posterior X-ray

	Volume (mL)[a]	Mean dose (cGy)[a]		*P* value[b]
		Pancreatic shield group	Non-pancreatic shield group	
Liver	8.51 ± 0.62	163.94 ± 16.60	135.37 ± 21.89	0.018
Stomach	3.78 ± 0.55	146.03 ± 32.82	95.96 ± 19.11	0.004
Right kidney	1.32 ± 0.13	127.87 ± 38.07	96.17 ± 39.33	0.151
Left kidney	1.22 ± 0.13	93.16 ± 21.77	38.94 ± 15.51	<0.001
Pelvic contour[c]	36.93 ± 3.74	265.33 ± 15.76	264.29 ± 16.11	0.905
Abdomino-pelvic contour[d]	171.43 ± 8.74	103.59 ± 4.20	106.23 ± 4.27	0.265
Pancreas	1.86 ± 0.23	53.33 ± 9.90	464.04 ± 8.37	<0.001

[a]The values are shown as the mean ± standard error.

[b]Student *t* test for mean doses of each contour volume, between the pancreatic shield and the non-pancreatic shield groups.

[c]The pelvic contour including all pelvic organs and skin area was delineated from the anal verge to the 18th slice location upward, with a 2-mm thickness.

[d]The abdomino-pelvic contour was delineated from the diaphragm to the anal verge level for integral dose assessment, as a substitute for whole body reflecting radiosensitive gastrointestinal area.

2. Change of body weight gain and blood glucose

After irradiation, the body weight gain failed to progress temporarily at Ep. For NPS-15-Gy group, it was even reduced temporarily leading to significant gap compared to that of NPS-5 Gy-group ($P < 0.001$, filled stars in Figure 3A). From the 5th week, the body weight was converted to a rapidly increasing pattern. With the passage of time, the dose-dependent body weight gap moved to from the NPS group to the PS group: at the 9th week ($P = 0.027$, empty stars in Figure 3A) and at Lp ($P = 0.028$, filled circles in Figure 3A). The blood glucose level decreased remarkably at Ep and it recovered gradually since then with an instant gap point between the PS-5-Gy and NPS-5-Gy groups at the 5th week ($P = 0.037$, empty circles in Figure 3B). Compared with the control group, the body weight gaps increased with time and this tendency was more severe in the high dose irradiation groups (Figure 4). For fasting blood glucose, there were no clear and consistent differences between each group and control group (Figure 5).

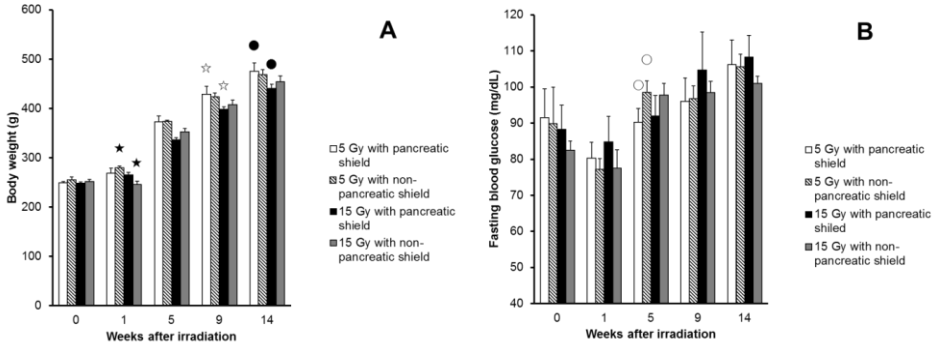

Figure 3. Changes in body weight (A) and fasting blood glucose (B) after irradiation. Data represent the mean and 95% confidence interval with six samples. Pairs of filled stars, empty stars, filled circles, and empty circles: $P < 0.05$. The asterisk indicates significance with the control group.

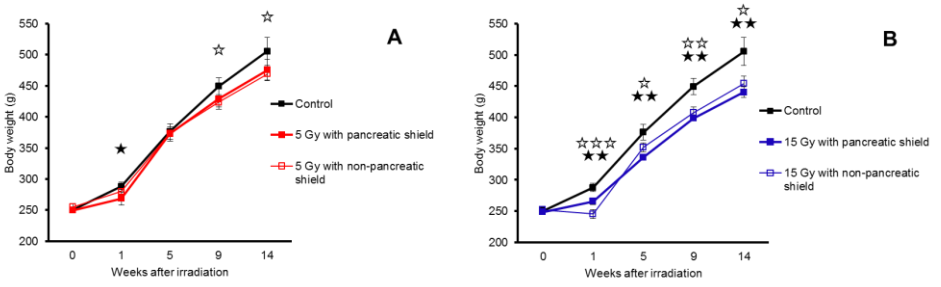

Figure 4. Changes in body weight for the pancreatic shield (PS) group and the non-pancreatic shield (NPS) group compared to sham irradiation (control) group after irradiation. (A) 5-Gy groups. (B) 15-Gy groups. Data represent the mean and 95% confidence interval with six samples. The field star indicates significance of PS group compared to control group ($^{\bigstar}P < 0.05$, $^{\bigstar\bigstar}P < 0.01$, $^{\bigstar\bigstar\bigstar}P < 0.001$). The empty star indicates significance of NPS group compared to control group ($^{\star}P < 0.05$, $^{\star\star}P < 0.01$, $^{\star\star\star}P < 0.001$).

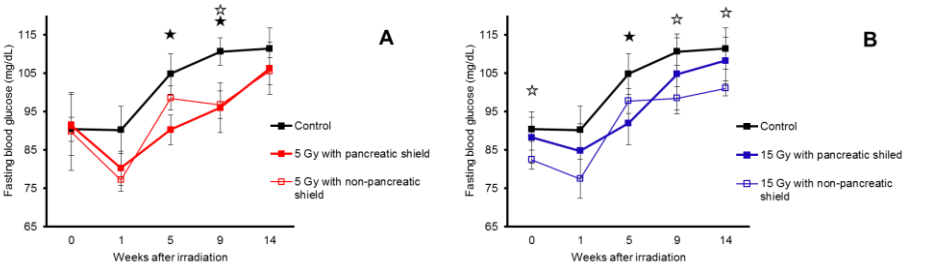

Figure 5. Changes in fasting blood glucose for the pancreatic shield (PS) group and the non-pancreatic shield (NPS) group compared to sham irradiation (control) group after irradiation. (A) 5-Gy groups. (B) 15-Gy groups. Data represent the mean and 95% confidence interval with six samples. The field star indicates significance of PS group compared to control group ($^{\bigstar}P < 0.05$). The empty star indicates significance of NPS group compared to control group ($^{\star}P < 0.05$).

3. Histopathologic findings by hematoxylin-eosin staining

At low magnification (×40), HE-stained rectum tissue did not show significant difference for each group and each crypt showed a uniform pattern without serious inflammatory injury. The mucosal structure such as the villous epithelial layers was relatively well preserved in all groups. Crypt depth, the thickness of the lamina propria, and vessel telangiectasis did not show definite difference. At high magnification (×400), some lymphocytes and apoptotic bodies were present with a few mitotic cells in the crypts, lamina propria, and

submucosal area mainly in high dose groups. Representative images are shown in Figure 6. A small infiltration of epithelial and interstitial inflammatory cells with crypt atrophy tendency was observed mainly in 15-Gy-Ep groups. The number of inflammatory cells tended to resolve at late phase. For 5-Gy groups, the apoptotic bodies and inflammatory cells were relatively difficult to observe and this pattern persisted to the late phase. Crypt atrophy tendency increased gradually from early phase to late phase and this tendency was similar in the 5 Gy and 15 Gy groups. There was no major difference between the PS and NPS groups in the presence of a few apoptotic bodies and granulocytes in the crypts with the condition of the same radiation dose and time point.

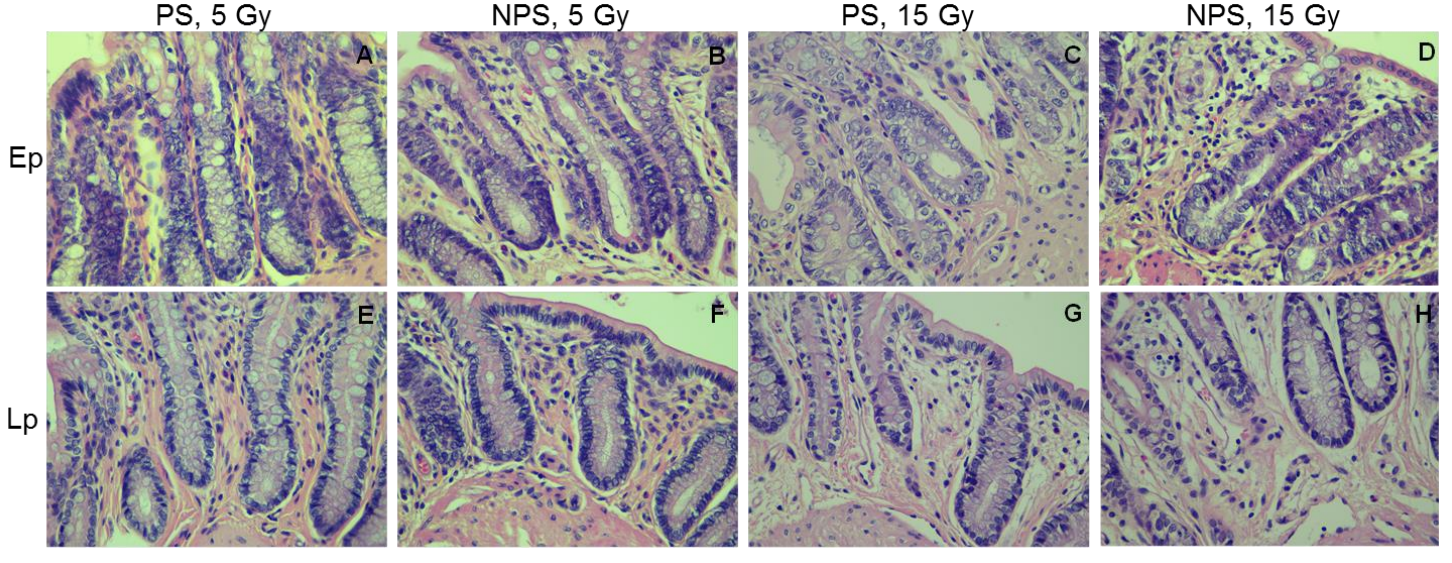

Figure 6. Histological changes in irradiated rectal mucosa on hematoxylin-eosin staining. Representative cross section images of the rectum tissue are shown for each group at the 1st week (early phase, Ep) and the 14th week (late phase, Lp) after irradiation. (A) Pancreatic shield (PS)-5-Gy-Ep group. (B) Non-pancreatic shield (NPS)-5-Gy-Ep group. (C) PS-15-Gy-Ep group. (D) NPS-15-Gy-Ep group. (E) PS-5-Gy-Lp group. (F) NPS-5-Gy-Lp group. (G) PS-15-Gy-Lp group. (H) NPS-15-Gy-Lp group. Magnification, ×400. Scale bar, 25 μm.

4. Apoptosis in rectal mucosa estimated by cleaved caspase-3 immunohistochemical staining

IHC staining was performed with antibody against cleaved caspase-3 to assess apoptosis in the crypt epithelial area. As shown in Figure 7, cleaved caspase-3 positive cells were detected for each group. At Ep, the mean number of cleaved caspase-3 positive cells per 100 cells of the PS-5-Gy, NPS-5-Gy, PS-15-Gy, and NPS-15-Gy groups was 1.30 ± 1.06, 1.11 ± 0.47, 2.58 ± 0.81, and 2.95 ± 1.67, respectively. At Lp, each value tended to increase to 2.55 ± 0.94, 2.90 ± 1.99, 3.73 ± 1.02, and 5.59 ± 1.39 for the same groups. Generally, the number of cleaved caspase-3 positive cells was more frequently detected at late phase compared to early phase and this time-dependent Ep-to-Lp increase was prominent in NPS-15-Gy group (P = 0.014, filled stars in Figure 8I). In terms of pancreatic radiation exposure, this cleaved caspase-3 expression tended to be relatively high in the NPS groups versus PS groups, especially in the 15-Gy group at Lp (P = 0.024, empty stars in Figure 7I). When compared with the control group, the degree of significant difference was stronger in the NPS groups than in the PS groups (Figure 7I).

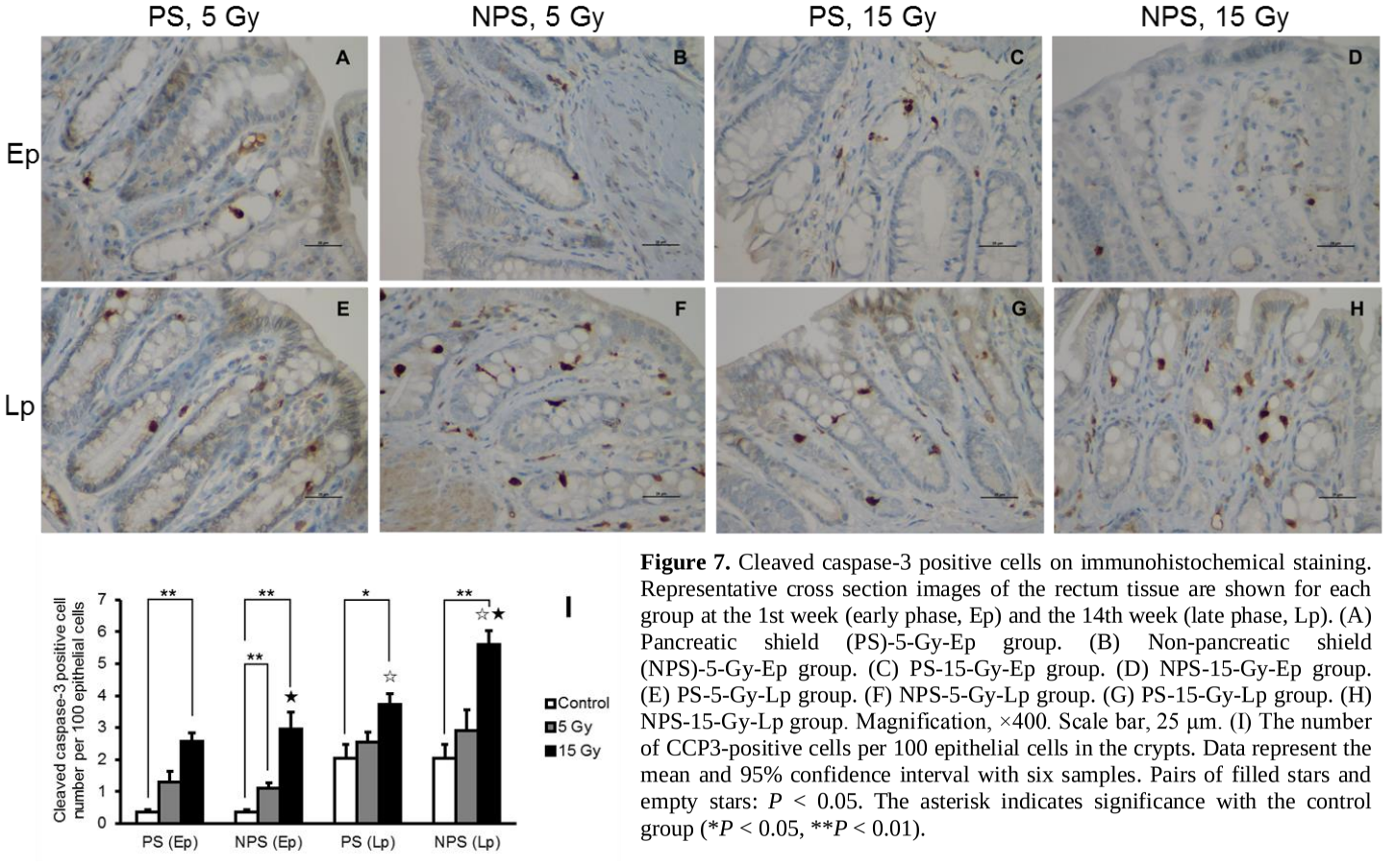

Figure 7. Cleaved caspase-3 positive cells on immunohistochemical staining. Representative cross section images of the rectum tissue are shown for each group at the 1st week (early phase, Ep) and the 14th week (late phase, Lp). (A) Pancreatic shield (PS)-5-Gy-Ep group. (B) Non-pancreatic shield (NPS)-5-Gy-Ep group. (C) PS-15-Gy-Ep group. (D) NPS-15-Gy-Ep group. (E) PS-5-Gy-Lp group. (F) NPS-5-Gy-Lp group. (G) PS-15-Gy-Lp group. (H) NPS-15-Gy-Lp group. Magnification, ×400. Scale bar, 25 μm. (I) The number of CCP3-positive cells per 100 epithelial cells in the crypts. Data represent the mean and 95% confidence interval with six samples. Pairs of filled stars and empty stars: $P < 0.05$. The asterisk indicates significance with the control group (*$P < 0.05$, **$P < 0.01$).

5. Fibrotic change in rectal mucosa and submucosa

Rectum tissue was stained with PR to assess mucosal and submucosal fibrosis with visualized single colored collagen deposition using image analysis software. Representative rectum tissue micrographs for each group stained with Masson's trichrome and PR are shown in Figure 8. As shown in Figure 8A to 8H, submucosal thickness did not show a significant difference among each group. However, when approached with a PR-positive area proportion, fibrosis became more intense toward the late phase. At Ep, the mean PR-positive area proportion of the PS-5-Gy, NPS-5-Gy, PS-15-Gy, and NPS-15-Gy groups was 26.01 ± 4.00%, 28.07 ± 3.09%, 29.36 ± 1.99%, and 28.39 ± 3.04%, respectively. At Lp, each value tended to increase to 30.62 ± 5.51%, 33.82 ± 2.36%, 33.70 ± 1.98%, and 35.71 ± 2.52% for the same groups. This Ep-to-Lp increase was observed in all groups except the PS-5-Gy group ($P < 0.05$, Filled stars, empty stars, and filled circles in Figure 8I). When compared with the sham-irradiated control groups, the difference of PR-positive proportion was more pronounced in the NPS groups than in the PS groups (Figure 8I).

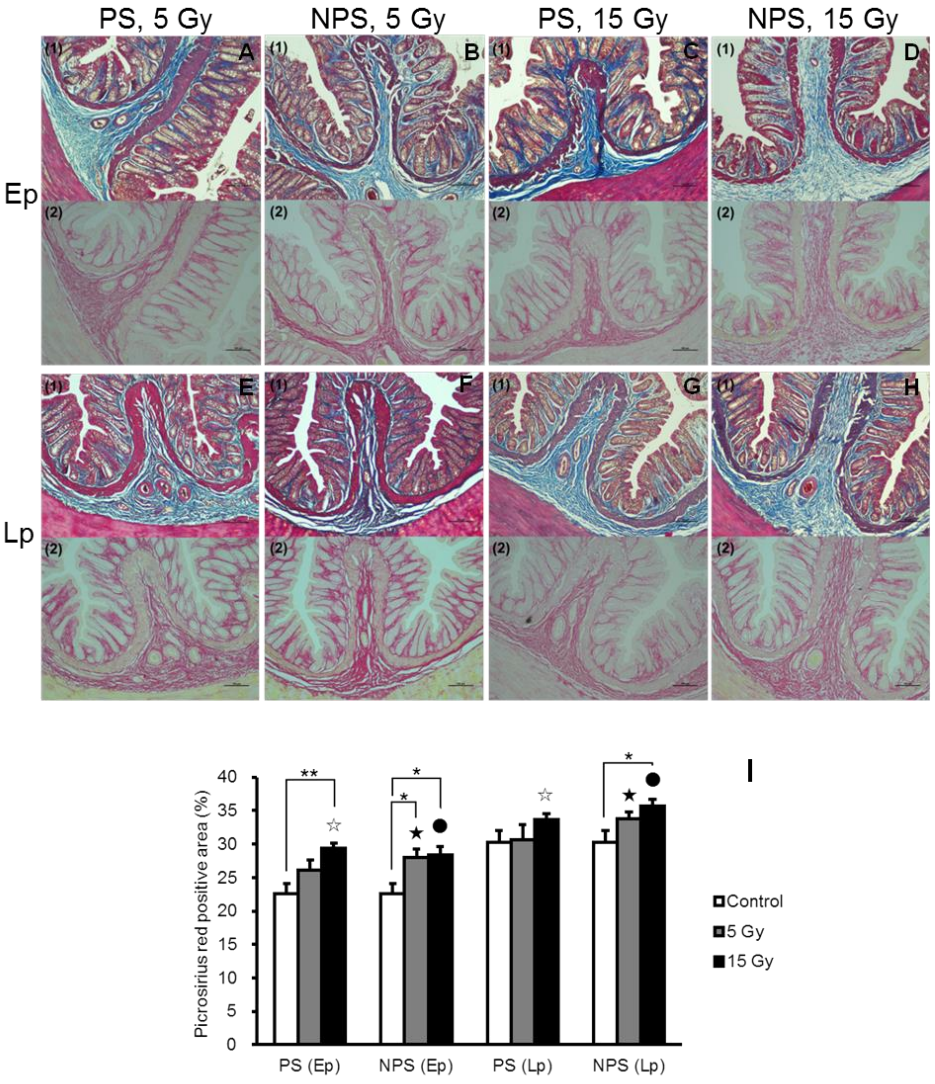

Figure 8. Fibrotic changes in rectal mucosa and submucosa on Picrosirius red (PR) staining. Representative cross section images of the rectum tissue stained by Masson's trichrome (1) and PR (2) are shown for each group at the 1st week (early phase, Ep) and the 14th week (late phase, Lp). (A) Pancreatic shield (PS)-5-Gy-Ep group. (B) Non-pancreatic shield (NPS)-5-Gy-Ep group. (C) PS-15-Gy-Ep group. (D) NPS-15-Gy-Ep group. (E) PS-5-Gy-Lp group. (F) NPS-5-Gy-Lp group. (G) PS-15-Gy-Lp group. (H) NPS-15-Gy-Lp group. Magnification, ×100. Scale bar, 100 μm. (I) The proportion of the PR positive area calculated in a defined mucosal and submucosal area of a representative villus. Data represent the mean and 95% confidence interval with six samples. Pairs of filled stars, empty stars, and filled circles: $P < 0.05$. The asterisk indicates significance with the control group (*$P < 0.05$, **$P < 0.01$).

6. mRNA expression of IL-6, HIF-1α, VEGF-A, and NF-κB

An increase in mRNA expression with dose escalation was observed for IL-6, especially in the PS group at Ep (P = 0.020, filled stars in Figure 9A). Generally, the expressions at Lp tended to decrease compared to those at Ep, with the same dose or pancreatic radiation exposure status. Comparing the PS groups with the NPS groups, the expressions of IL-6 and NF-κB, which are thought to be related to inflammation, tended to be stronger in the NPS groups than those of the PS groups irrespective of time point although the statistical significance was not sufficient. When assessed by the number of significant Ep-Lp decrease pairs, NF-κB (4 pairs) showed the greatest tendency and the PS groups (7 pairs) had more numbers than NPS groups (4 pairs). There were cases that the decrease in mRNA expression in Lp was more severe than in the control group, which was also most prominent in NF-κB (Figure 9).

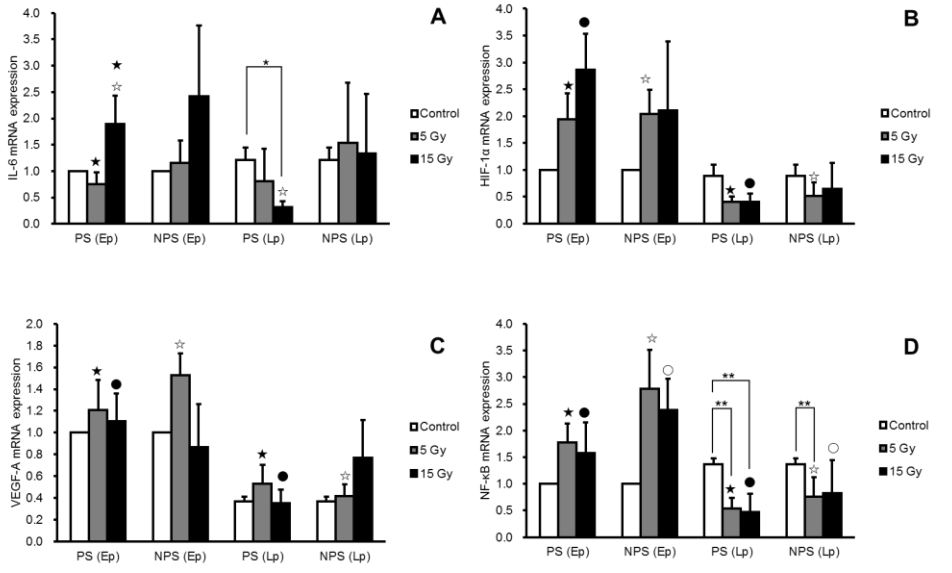

Figure 9. Relative mRNA expression (real time PCR using rat-specific primers) compared to one control subject at the 1st week (early phase, Ep) and the 14th week (late phase, Lp) after irradiation for each group. (A) Interleukin-6 (IL-6). (B) Hypoxia-inducible factor (HIF)-1α. (C) Vascular endothelial growth factor (VEGF)-A. (D) Nuclear factor (NF)-κB. Data represent the mean and 95% confidence interval of the results of three independent experiments, each with six samples. A significant Ep-Lp decrease pairs ($P < 0.05$) are denoted as filled stars, empty stars, filled circles, and empty circles. The asterisk indicates significance with the control group (*$P < 0.05$, **$P < 0.01$).

IV. DISCUSSION

The aim of the present study was to confirm the concept of inter-organ effect in radiation-induced rectal toxicity in conjunction with pancreatic radiation exposure. The iCPR method was used to modulate pancreatic radiation exposure and inter-organ effect between the pancreas and the rectum. Histopathologic findings of rectal mucosa and submucosa were accompanied by body weight and fasting blood glucose. In the apoptosis-dominant dose range,

apoptosis and fibrosis in the rectal mucosa or submucosa showed consistent patterns under specific conditions in the midst of radiation dose and follow-up period-dependent relationship.

Radiation toxicity of one organ can be influenced by the status of simultaneously irradiated adjacent other organs.[13, 14, 18] Pancreatic radiation exposure also can be a part in the process of GIT toxicity.[14, 16] However, there have not been sufficient follow-up studies due to the technical difficulty in separately irradiating each organ in the abdomen. It is technically impossible to modulate pancreatic radiation exposure and the upper GIT-specific radiation damage separately with proper control groups because the upper abdomen is composed of the pancreas and surrounding bulky GITs in the central portion. In addition, GIT toxicity can be aggravated by the proteolytic activity of the pancreatic enzymes.[19-21] The rectum, which is free from pancreatic enzyme influence and located far from the pancreas, was estimated to be valid for assessing pancreatic radiation exposure in GIT radiotoxicity. The iCPR method allowed for objectivity by targeting pancreatic enzyme-independent rectum, as an alternative option to pancreatic enzyme-dependent upper GIT. Pancreatic radiation exposure-unaffected dose balance is another issue. Our dosimetric comparison between the PS and the NPS showed the feasibility of maintaining dose balance in the area around the pancreas regardless of pancreatic radiation exposure.

Previous studies showed >25 Gy was required to induce rodent GIT

inflammation.[22, 23] This dose level may trigger secondary reactions, making it difficult to establish a clinical situation-reflected GIT toxicity model. Difficulties are more pronounced in pancreatic histologic change-related cases because pancreatic radioresistance is much higher.[13, 24] In addition, the dose level of pancreatic histologic injury can result in the problem of unfair assessment which originated from the fundamental radiosensitivity difference between the GIT and the pancreas. Our apoptosis-dominant dose level of 5–15 Gy was derived focusing on primary GIT toxicity with minimized inflammatory reactions.

As expected in our study, there was no difference between groups in the microstructure of the pancreas due to the histologic radioresistance (data not shown). However, relatively low-level effect to the pancreas may disturb systemic nutritional status. According to Sarri et al.,[25] 10-Gy irradiation to the entire rat abdomen resulted in rapid normoinsulinemic hypoglycemia without definitive pancreatic histologic change, which may imply impaired insulin secretion from the islet cells. This hypothesis was applied in our study, and pancreatic radiation exposure-related malnutrition may have influenced histologic changes of the rectal mucosa.

The value of serum amylase/lipase was measured in our study. However, there was no difference in each irradiation group (data not shown). This may be due to the ill-defined histological characteristics of the pancreatic injury and the GIT injury effect on serum data. On CT-based simulation, the dose exposure to

liver, stomach, and left kidney was relatively high in the PS irradiation group compared to that in the NPS group, even in well-balanced irradiation conditions (Table 2). NPS radiation dose was relatively low compared to PS radiation dose in many contour volumes, and yet, considerable histological changes were observed in the rectal mucosa, which indicates the suitability of the iCPR method. A recent clinical study revealed possible compromised serum amylase/lipase profiles by radiation. However, it may not be possible to generalize those results, since the data in that study was confined to the amylase/lipase profiles and the radiation dose distributions in abdominal organs were not specified at all.[17] Consequently, at this time, the most reliable parameter for pancreatic radiation exposure can be dosimetric data.

In the aspect of body weight profile, there seemed to be a dose-dependency in the NPS irradiation group at Ep (Figure 3A and Figure 4). Blood glucose levels were nonspecific to pancreatic radiation exposure and there was no sign of diabetes (Figure 3B and Figure 5). This seems to be due to the fact that our radiation dose level was not enough to affect islet cells. Although there was no direct difference in parametric indices between the PS and NPS groups, the changing patterns of body weight according to radiation dose level indicated differences to some extent. This pattern was partly similar to apoptosis-related effects in cleaved caspase-3 IHC staining. The pancreatic radiation exposure-related GIT toxicity pattern was confirmed for cleaved caspase-3 expression under certain conditions especially in 15-Gy-Lp group (Figure 7I). The number of cleaved caspase-3 positive cells showed a continuous increase

toward Lp including the natural increment of the sham-irradiated control groups (Figure 7I).

Interestingly, it should be noted that the time-dependent natural increase in rectal mucosal apoptosis was not negligible. As a whole, changes in gut bacteria status, intestinal immune environment, or other cleaved caspase-3 associated tissue responses, are thought to be influential in the cell death regulation system.[26, 27] In addition, the possibility of other external factors can be considered during the radiation toxicity process. As an extreme example, burns can be a major cause of gut mucosal atrophy, which was shown to occur in multifactorial processes.[28] Histophysiologic properties of the rectal mucosa different from jejunum, ileum, or proximal colon, cannot be overlooked, although the exact contributions are unknown. According to Romany et al.,[29] cleaved caspase-3 activation decreased 9 weeks after fractionated abdominal irradiation in the jejunal and colonic crypts, which was not the case for the rectal mucosa in our study. Other problems such as bowel motility and intestinal mucosal stress due to physical stimulation can also be considered, which can be linked to the flow of time course. In fact, in our study, the rectum had bulky stool during the extraction of the tissue in many cases, even though the 18-h fasting was always maintained, which might have affected additional mucosal damage. Research design that can control these factors will be needed in the future.

Fibrotic change increased with the passage to the late phase regardless of

radiation dose. The fibrosis progressed more in the NPS group than in the control group. However, these results were not clear enough to be generalized. Rather, the fibrosis of the sham-irradiated control group was noticeable as a natural increase over time to the late phase. In addition, in this study, it was shown that low radiation dose could be a factor causing fibrosis after a certain period of time. Fibrosis is known to occur even with acceptably low doses.[24] In a previous study as a similar situation, there was an overall increase in fibrotic changes not only in the case of high radiation dose but also in the presence of toxicity-reducing factors such as the extension of overall treatment time.[30]

Even though a histologic inflammatory reaction was not apparent, differential expression of inflammation-related mRNA expression was observed. IL-6 reflected a typical dose-dependency as in the previous studies.[4, 7] The mRNA expression of IL-6, HIF-1α, NF-κB, and VEGF-A tended to increase at Ep and decrease at Lp. In particular, the expressions of IL-6 and NF-κB, which are thought to be related to inflammation, tended to be strong in the NPS groups irrespective of time point. The PS irradiation group had a larger number of inflammatory genes that showed a decrease in expression from Ep to Lp (Figure 9). This might be related to tissue recovery process such as rectal mucosa regeneration. Despite this tendency, however, the lack of significance in other cytokines other than IL-6 appears to be due to relatively heterogeneous tissue sample for qPCR. These data were not from the rectal mucosa alone but from the whole rectum, which was an attempt to investigate the overall aspect of rectal toxicity as an adjunctive approach in addition to histologic and IHC

analysis. Fundamentally, simple approaches such as apoptosis, fibrosis, or inflammation have limitations in radiation toxicity assessment. In view of embracing conflicting results of each method, the introduction of a proper scoring system can be considered. Apoptosis-inducible radiation may increase or decrease the regeneration capacity of the GIT itself, which was represented by various histological results with the possibility of a subtle effect of pancreatic radiation exposure.

This study had some limitations stemming from the use of the first attempted experimental approach. First, our *in vivo* study was based on a macroscopic approach, which needs to be complemented by a suitable *in vitro* model with in-depth molecular biological analysis. Second, it was difficult to guarantee that the planned radiation dose was transmitted to the pancreas entirely, due to the respiratory motions in the abdomen. To minimize this issue, we applied more strict dosimetric conditions for PS irradiation. Targeted radiation of rectum and pancreas by precision small animal irradiation platforms can help determine the role of the pancreas in rectal radiation toxicity more accurately in the future studies. Third, simple approaches such as apoptosis or fibrosis had limitations in identifying the role of the pancreas fundamentally in toxicity analysis. A follow-up study will require more sophisticated data derived through more diversified approaches.

V. CONCLUSION

In conclusion, the iCPR method is feasible in assessing multi-organ effect in clinical situation-reflected *in vivo* study. PS irradiation is helpful in reducing negative factors of GIT toxicity from the various perspectives of multi-organized approaches such as body weight, apoptosis, and fibrosis. Above all, it is noteworthy that PS resulted less toxicity tendency despite the same rectal dose and more unfavorable dosimetric conditions compared to NPS.

REFERENCES

1. Polistena A, Johnson LB, Ohiami-Masseron S, Wittgren L, Back S, Thornberg C, et al. Local radiotherapy of exposed murine small bowel: apoptosis and inflammation. BMC Surg 2008;8:1.
2. Nagtegaal ID, Gaspar CG, Peltenburg LT, Marijnen CA, Kapiteijn E, van de Velde CJ, et al. Radiation induces different changes in expression profiles of normal rectal tissue compared with rectal carcinoma. Virchows Arch 2005;446:127-35.
3. Bowen JM, Gibson RJ, Keefe DM. Animal models of mucositis: implications for therapy. J Support Oncol 2011;9:161-8.
4. Ong ZY, Gibson RJ, Bowen JM, Stringer AM, Darby JM, Logan RM, et al. Pro-inflammatory cytokines play a key role in the development of radiotherapy-induced gastrointestinal mucositis. Radiat Oncol 2010;5:22.
5. Okunieff P, Cornelison T, Mester M, Liu W, Ding I, Chen Y, et al. Mechanism and modification of gastrointestinal soft tissue response to radiation: role of growth factors. Int J Radiat Oncol Biol Phys 2005;62:273-8.
6. Linard C, Marquette C, Mathieu J, Pennequin A, Clarencon D, Mathe D. Acute induction of inflammatory cytokine expression after gamma-irradiation in the rat: effect of an NF-kappaB inhibitor. Int J Radiat Oncol Biol Phys 2004;58:427-34.
7. Rentea RM, Lam V, Biesterveld B, Fredrich KM, Callison J, Fish BL, et

al. Radiation-induced changes in intestinal and tissue-nonspecific alkaline phosphatase: implications for recovery after radiation therapy. Am J Surg 2016;212:602-8.

8. Bentzen SM. Preventing or reducing late side effects of radiation therapy: radiobiology meets molecular pathology. Nat Rev Cancer 2006;6:702-13.

9. Paris F, Fuks Z, Kang A, Capodieci P, Juan G, Ehleiter D, et al. Endothelial apoptosis as the primary lesion initiating intestinal radiation damage in mice. Science 2001;293:293-7.

10. Liu Y, Kudo K, Abe Y, Aoki M, Hu DL, Kijima H, et al. Hypoxia expression in radiation-induced late rectal injury. J Radiat Res 2008;49:261-8.

11. Bae BK, Kang MK, Kim JC, Kim MY, Choi GS, Kim JG, et al. Simultaneous integrated boost intensity-modulated radiotherapy versus 3-dimensional conformal radiotherapy in preoperative concurrent chemoradiotherapy for locally advanced rectal cancer. Radiat Oncol J 2017;35:208-16.

12. Lee DS, Woo JY, Kim JW, Seong J. Re-Irradiation of Hepatocellular Carcinoma: Clinical Applicability of Deformable Image Registration. Yonsei Med J 2016;57:41-9.

13. Ahmadu-Suka F, Gillette EL, Withrow SJ, Husted PW, Nelson AW, Whiteman CE. Pathologic response of the pancreas and duodenum to experimental intraoperative irradiation. Int J Radiat Oncol Biol Phys 1988;14:1197-204.

14. Zook BC, Bradley EW, Casarett GW, Rogers CC. Pathologic effects of fractionated fast neutrons or photons on the pancreas, pylorus and duodenum of dogs. Int J Radiat Oncol Biol Phys 1983;9:1493-504.

15. Nam H, Lim DH, Kim S, Kang WK, Sohn TS, Noh JH, et al. A new suggestion for the radiation target volume after a subtotal gastrectomy in patients with stomach cancer. Int J Radiat Oncol Biol Phys 2008;71:448-55.

16. Gemici C, Sargin M, Uygur-Bayramicli O, Mayadagli A, Yaprak G, Dabak R, et al. Risk of endocrine pancreatic insufficiency in patients receiving adjuvant chemoradiation for resected gastric cancer. Radiother Oncol 2013;107:195-9.

17. Wydmanski J, Polanowski P, Tukiendorf A, Maslyk B. Radiation-induced injury of the exocrine pancreas after chemoradiotherapy for gastric cancer. Radiother Oncol 2016;118:535-9.

18. Ghobadi G, van der Veen S, Bartelds B, de Boer RA, Dickinson MG, de Jong JR, et al. Physiological interaction of heart and lung in thoracic irradiation. Int J Radiat Oncol Biol Phys 2012;84:e639-46.

19. Wang J, Zheng H, Sung CC, Hauer-Jensen M. The synthetic somatostatin analogue, octreotide, ameliorates acute and delayed intestinal radiation injury. Int J Radiat Oncol Biol Phys 1999;45:1289-96.

20. Lloyd-Still JD, Uhing MR, Arango V, Fusaro A, Kimura RE. The effect of intestinal permeability on pancreatic enzyme-induced enteropathy in the rat. J Pediatr Gastroenterol Nutr 1998;26:489-95.

21. Kimura RE, Arango V, Lloyd-Still J. Indomethacin and pancreatic enzymes synergistically damage intestine of rats. Dig Dis Sci 1998;43:2322-32.

22. Blirando K, Milliat F, Martelly I, Sabourin JC, Benderitter M, Francois A. Mast cells are an essential component of human radiation proctitis and contribute to experimental colorectal damage in mice. Am J Pathol 2011;178:640-51.

23. Kim KT, Chae HS, Kim JS, Kim HK, Cho YS, Choi W, et al. Thalidomide effect in endothelial cell of acute radiation proctitis. World J Gastroenterol 2008;14:4779-83.

24. Berthrong M. Pathologic changes secondary to radiation. World J Surg 1986;10:155-70.

25. Sarri Y, Conill C, Verger E, Tomas C, Gomis R. Effects of single dose irradiation on pancreatic beta-cell function. Radiother Oncol 1991;22:143-4.

26. Ferreira MR, Muls A, Dearnaley DP, Andreyev HJ. Microbiota and radiation-induced bowel toxicity: lessons from inflammatory bowel disease for the radiation oncologist. Lancet Oncol 2014;15:e139-47.

27. Nakahashi-Oda C, Udayanga KG, Nakamura Y, Nakazawa Y, Totsuka N, Miki H, et al. Apoptotic epithelial cells control the abundance of Treg cells at barrier surfaces. Nat Immunol 2016;17:441-50.

28. Wu X, Woodside KJ, Song J, Wolf SE. Burn-induced gut mucosal homeostasis in TCR delta receptor-deficient mice. Shock 2004;21:52-7.

29. Stansborough RL, Bateman EH, Al-Dasooqi N, Bowen JM, Keefe

DMK, Yeoh ASJ, et al. Fractionated abdominal irradiation induces intestinal microvascular changes in an in vivo model of radiotherapy-induced gut toxicity. Support Care Cancer 2017;25:1973-83.

30. Langberg CW, Sauer T, Reitan JB, Hauer-Jensen M. Relationship between intestinal fibrosis and histopathologic and morphometric changes in consequential and late radiation enteropathy. Acta Oncol 1996;35:81-7.

ABSTRACT (IN KOREAN)

방사선 유발성 직장 점막 세포사멸과 섬유화에 대한 췌장, 직장 동시 국소 방사선 조사의 영향

<지도교수 이 창 걸>

연세대학교 대학원 의학과

유 세 환

목적: 췌장에 대한 방사선 노출은 위장관 방사선 독성에 부정적인 영향을 미칠 수 있다. 췌장은 혈당, 영양 및 대사 관련 작용에서 영향을 미침으로써 위장관 시스템의 치유 과정에서 방사선 장독성에 영향을 줄 수 있다. 따라서 췌장에 대한 방사선 영향에 따라 위장관 독성을 분석하고 장기 상호 간의 영향 개념에 따라 방사선 독성 제어 시스템을 검증하는 것이 필요하다. 방사선 유발성 위장관 독성 평가를 함에 있어 위장관과 췌장 상호 관련성 개념을 확인하기 위해 췌장 방사선 영향 관련 쥐 동물 모델을 적용하였다.

재료 및 방법: 8주령 수컷 *Sprague Dawley* 쥐에게 고에너지

방사선을 조사하였다. 췌장 방사선 영향에 따른 위장관 독성 영향을 검증하기 위해 방사선 조사를 상복부와 하복부로 나누어 '췌장, 직장 동시 방사선 조사' 기법을 적용 하였다. 이 때 상복부에는 췌장이, 하복부에는 직장이 포함되도록 하였다. 이 기법은 조사받는 부피가 일정하게 유지되는 적절한 프로토콜을 제공할 수 있도록 고안되었다. 상복부 방사선 조사는 췌장차폐(Pancreatic shield, PS)와 비췌장차폐(Non-pancreatic shield, NPS)로 분류하였다. 5 Gy와 15 Gy 조사 후 1주(초기 단계, Early phase, Ep), 14주(후기 단계, Late phase, Lp) 시점에 체중과 공복혈당과 함께 직장 조직을 분석하였다. 조직 병리학은 hematoxylin & eosin (HE), Masson 's trichrome, Picrosirius red (PR) 염색으로 시행하였다. 직장 점막에서 세포사멸을 평가하기 위한 면역조직화학 염색은 cleaved caspase-3 항체로 수행하였다. 방사선량, 위장관의 급성, 만성 독성 및 췌장 방사선 영향 등을 고려하면서 염증 또는 섬유화 표지자로서 interleukin (IL)-6, hypoxia-inducible factor (HIF)-1α, vascular endothelial growth factor (VEGF)-A, and nuclear factor (NF)-κB의 mRNA 발현을 분석하였다.

결과: 체중 증가는 조사 후 1주째 시점에 더디게 나타났으며 이는 NPS-5-Gy군 대비 NPS-15-Gy군에서 두드러졌다($P < 0.001$). 혈당치는 초기 단계에서 감소 후 후기 단계로 가면서 점차 증가하였다. 체중 증가와 혈당 변화 모두 초기 단계에서 일시적으로 감소 추세를 나타냈다는 측면에서 유사한 양상을 보였는데 이는

NPS-15-Gy군에서 전형적으로 나타났다. HE 염색에서 15-Gy 조사군의 염증 반응이 주로 초기 단계에서 현저하였다. 직장 점막의 세포사멸은 cleaved caspase-3 양성 세포의 수로 평가하였다. 전체적으로, cleaved caspase-3 양성 세포의 수는 초기 단계에 비해 후기 단계에서 더 많이 감지되었고, 이러한 초기 대비 후기 단계에서의 증가는 NPS-15-Gy군에서 현저하였다(P = 0.014). 후기 단계의 15-Gy 조사군에 국한시켰을 경우, cleaved caspase-3 발현은 PS군에 비해 NPS군에서 우세하였다(P = 0.024). 점막하 섬유화의 정량적 평가는 PR 염색 조직 상 전체 융모막에서 콜라겐 침착이 차지하는 면적의 비율로 하였다. PS군과 NPS군 간에 유의한 차이는 없었지만 점막하 섬유화는 전반적으로 시간의 흐름에 따라 진행되는 양상이었으며 이러한 초기 대비 후기 단계에서의 증가는 PS-5-Gy군을 제외한 모든 군에서 관찰되었다. 콜라겐 침착 자체는 방사선이 조사되지 않은 대조군과 비교했을 경우 PS군보다 NPS군에서 더 큰 경향을 나타내었다. 일반적으로 IL-6, HIF-1α, VEGF-A 및 NF-κB의 mRNA 발현은 동일한 방사선 투여 량 또는 췌장 차폐 상태 기준으로, 초기 단계에서 현저했다가 이후 회복되는 경향을 보였다. 이 중 후기 단계에서의 IL-6 mRNA 발현은 전형적으로 방사선량에 비례하였다(P = 0.020).

결론: 본 연구에서는 방사선에 의한 직장 독성을 췌장에 대한 방사선 영향과 연관 지어 고찰하였다. PS군과 NPS군의

조직병리학적, 생화학적 변화는 양군간에 현저한 차이 없이 방사선량과 시기별 특색을 가지면서 변화하였다. 본 연구의 동물모델에 의하면 염증반응은 주로 초기 단계에, 섬유화와 함께 동반되는 세포사멸은 주로 후기 단계에 발생하였다. 섬유화는 방사선을 조사 받지 않은 대조군과 비교 시 예상보다 이른 시기에 발생할 가능성이 있는 것으로 생각되었으며 이는 콜라겐 침착의 증가로 확인되었다. PS와 NPS군 간에 직접적인 독성 차이는 현저하다고 볼 수는 없었다. 하지만, 본 연구에서 적용한 췌장차폐는 직장점막의 방사선 독성에서 방사선량 의존성과 시간 연관성의 흐름에서 변수로 작용할 가능성이 있으며, 이는 위장관 방사선 독성 평가에서 장기 상호 간 영향을 고려한 접근법의 필요성을 의미한다.

핵심되는 말: 방사선 독성, 위장관, 췌장, 영양 상태